RSC Advances

PAPER

View Article Online
View Journal | View Issue

Cite this: *RSC Adv.*, 2025, **15**, 41699

Fine structure investigation and laser cooling study of the LaH molecule

Nariman Abu El Kher, [a] Nayla El-Kork, *[ab] Nissrin Alharzali,†[a] Joumana Assaf [cd] and Mahmoud Korek [e]

A theoretical feasibility study of the spin–orbit laser cooling of the molecule LaH has been performed based on a complete active space self-consistent field (CASSCF)/MRCI *ab initio* calculation with Davidson correction in the $\Lambda^{(\pm)}$ and $\Omega^{(\pm)}$ representations. The adiabatic potential energy curves and spectroscopic constants have been investigated for the considered electronic states. The small value of the equilibrium positions difference ΔR_e between the ground and the electronic states $X^3\Sigma_{0+}$, $(1)^3\Pi_{0+}$, and $(1)^3\Delta_1$ predicts the candidacy of the molecule LaH for direct laser cooling between the first two states with the intermediate state $(1)^3\Delta_1$. The calculation of the diagonal Franck–Condon factors, the short radiative lifetime, and the experimental parameters (slowing distance, Doppler and recoil temperature, …) suggest that the molecule LaH is a good candidate for Doppler laser cooling, and a corresponding laser cooling scheme is presented.

Received 17th April 2025
Accepted 8th August 2025

DOI: 10.1039/d5ra02708j

rsc.li/rsc-advances

1. Introduction

The development of techniques for producing, trapping, and controlling ultracold molecules in the gas phase has marked a major milestone in physics, attracting significant research interest over the years. Ultracold molecules offer a wide range of potential applications, including precision measurements,[1,2] simulation of solid-state systems,[3,4] quantum information processing,[5] and the control of chemical reactions at ultracold temperatures.[6] Numerous studies have explored a range of diatomic polar molecules and ions, including hydrogen, as potential candidates for laser cooling. These include alkaline-earth-metal monohydrides[7] (such as BeH, MgH, CaH, SrH, and BaH), transition metal hydrides (such as AgH,[8] CuH,[9] and AuH[10]), and other molecular systems (like CH,[11] AlH and AlF,[12] BH^+ and AlH^+[13]). Our recent work reported HfH[14] as a highly promising candidate for experimental laser cooling.

In general, the study of the electronic structure of molecules with open d and f orbitals (partial occupation), such as transition metals hydrides and Lanthanides hydrides, presents a major challenge for both theorists and experimentalists due to the significant electron–degeneracy correlations[15–17] involved. The formation of chemical bonds arising from d-electrons poses a significant difficulty for theorists, as accurately modeling these molecules requires considering relativistic effects and spin–orbit coupling.[18] Besides their importance in theoretical chemistry, the group of lanthanides hydrides such as LaH plays a critical role in various fields, such as astrophysics (since hydrogen is the most abundant element in the universe, LaH is found in the spectra of sunspots and cool stars),[19] catalysis,[20] organometallic chemistry,[21] and electron's electric dipole moment (EDM) measurements.[22] The electronic structure of the LaH molecule has been experimentally examined in the literature,[23–28] with previous theoretical studies provided in ref. 29–31. Recently, Assaf *et al.*[32] conducted a comprehensive theoretical study of the LaH molecule in both $\Lambda^{(\pm)}$ and $\Omega^{(\pm)}$ representations. Nevertheless, the study of the laser-cooling candidacy of the LaH molecule has never been explored.

This paper presents a spin–orbit coupling theoretical calculation and laser cooling investigation of the LaH molecule based on Assaf *et al.*'s previous work.[32] Additionally, we investigated the diagonal Frank-Condon factors (FCFs) and the radiative lifetimes (τ) for the two transitions $X^3\Sigma_{0+}$–$(1)^3\Pi_{0+}$ and $(1)^3\Delta_1$–$(1)^3\Pi_{0+}$, where $(1)^3\Delta_1$ is an intermediate state between $X^3\Sigma_{0+}$ and $(1)^3\Pi_{0+}$ states. The branching ratios of the vibrational transitions $R_{v'v}$ have been calculated along with the number of cycles (N) for photon absorption/emission and the slowing distance L, which falls within the practical experimental limits. A laser cooling scheme with an intermediate state is presented.

2. Computational approach

In this paper, we have employed the state-averaged Complete Active Space Self-Consistent Field (CASSCF) method, followed

[a]Department of Physics, Khalifa University, P.O. Box 127788, Abu Dhabi, United Arab Emirates. E-mail: nayla.elkork@ku.ac.ae
[b]Space and Planetary Science Center, Khalifa University, Abu Dhabi, United Arab Emirates
[c]Doctoral School of Sciences and Technology, Lebanese University, Hadath, Lebanon
[d]Center for Educational Research and Development, CERD, Sin El Fil, Lebanon
[e]Faculty of Science, Beirut Arab University, Riad El Solh, Beirut 1107 2809, Lebanon
† Current affiliation: Department of Physical and Theoretical Chemistry at Comenius University in Bratislava- Slovakia.

by Multi-Reference Configuration Interaction (MRCI) calculations with Davidson correction (+Q) to study the electronic structure of the LaH molecule. The high-level *ab initio* computations were conducted with the MOLPRO[33] software, utilizing the GABEDIT[34] graphical user interface. Due to the large number of electrons in the lanthanum atom ($_{57}$La), selecting appropriate basis sets that accurately describe its electronic structure is challenging. Given that this study focuses on the laser cooling of the LaH molecule, we are particularly interested in its ground state and the first two excited states $(1)^3\Delta$ and $(1)^3\Pi$. To ensure high-precision calculations while accounting for spin–orbit coupling effects, we examined various basis sets based on previously published data.

In 2014, Mahmoud and Korek[31] reported theoretical calculations on the low-lying electronic states of the LaH molecule, both with and without spin–orbit coupling, using the CASSCF/MRCI method. They employed the SBKJC-VDZ (ECP46MHF) valence double-zeta[35] basis set for lanthanum, which incorporates a relativistic effective core potential, and the augmented correlation-consistent polarized valence quadruple-zeta (aug-cc-pVQZ) basis set for hydrogen.[36] With the 12 electrons explicitly considered for the LaH molecule in the C_{2v} symmetry, the authors performed the calculations with different valence electrons (2, 6, 8, and 10 valence electrons) to check their influence on the values of the transition energy with respect to the ground state minimum (T_e). Their findings indicated that when two or six valence electrons were included, the $(1)^3\Delta$ state was lower in energy than the $(1)^3\Pi$ state, consistent with the experimentally observed order of states.[25] However, for a higher number of valence electrons, the $(1)^3\Pi$ state became lower in energy than the $(1)^3\Delta$ state. Recently, Assaf *et al.*[32] determined the spectroscopic constants of the LaH molecule using the quasi-relativistic effective core potential (ECP28-MWB) basis set[37,38] for lanthanum. In this approach, lanthanum is described by replacing its 28 inner-core electrons with the effective core potential, while the remaining 29 electrons are explicitly represented by the ANO Gaussian basis set with a contraction scheme of (14s, 13p, 10d, 8f, 6g)/[6s, 6p, 5d, 4f, 3g].[37,38] The hydrogen single electron is treated with the augmented correlation-consistent polarized valence quadruple-zeta (aug-cc-pVQZ) basis set,[36] contracted as (7s, 4p, 3d, 2f)/(5s, 4p, 3d, 2f). The authors calculated the low-lying excited states in both $\Lambda^{(\pm)}$ and $\Omega^{(\pm)}$ representations and determined the corresponding spectroscopic constants. Their results showed strong agreement with experimental data. Motivated by this, we employ the same basis sets (ECP28-MWB in conjunction with ANO Gaussian basis set[37,38] for La and aug-cc-pVQZ[36] for H) as well as the all-electron approach described by Assaf *et al.*[32] to carry out our own calculations, both with and without spin–orbit coupling (S.O.C) effects, aiming for a more accurate analysis relevant to laser cooling of the LaH molecule.

To assess the reliability of the employed pseudopotentials and basis sets, we have performed the calculations of our study using a benchmark of basis sets B_1–B_5, along with literature values, all compared with experimental data as shown in Table 1. The B_1 set employs the pseudopotential ECP28MWB[37,38] for lanthanum with a (s, p, d, f, g) ANO Gaussian basis set,[37,38] combined with the aug-cc-pVQZ[36] (s, p, d, f) basis for hydrogen. The B_2 set retains the same basis for La as in B_1 but uses a higher-level aug-cc-pV5Z[39] (s, p, d, f) basis for H. The B_3 set again uses ECP28MWB[37,38] for La but combines it with the smaller aug-cc-pVTZ[39] (s, p, d) basis for H. In contrast, B_4 and B_5 utilize the ECP46MWB[35,40] pseudopotential for La, where Lanthanum is described as a system of 46 inner electrons, and the remaining 11 electrons are represented by the corresponding basis set ECP46MWB-II ((6s6p5d)/[4s4p4d] + 2s1p1d).[35,41,42] The active space of C_{2v} point group symmetry contains 5σ (La: $5d_{+2}$, $6p_0$, $5d_0$; H: 1 s, 2 s), 2π (La: $5d_{+1}$, $6p_{+1}$; H: 0), 1δ (La: $5d_{-2}$; H: 0) molecular orbitals and are distributed into the irreducible representation as $5A_1$, $2B_1$, $2B_2$, and $1A_2$, denoted by [5, 2, 2, 1]. A CASSCF calculation was performed with two valence electrons from LaH distributed over the ten active orbitals. B_4 combines ECP46MWB[35,40] with aug-cc-pV5Z[39] (s, p, d, f) for H, while B_5 pairs it with aug-cc-pVQZ[36] (s, p, d, f) for H. Across all considered electronic states in the $\Lambda^{(\pm)}$ representation $X^1\Sigma^+$, $(1)^3\Delta$, and $(1)^3\Pi$, this benchmarking enables a detailed assessment of the sensitivity of spectroscopic constants: the equilibrium bond length R_e, the transition energy with respect to the ground state minimum T_e, the harmonic frequency ω_e, and the anharmonicity constant $\omega_e x_e$ to the choice of basis sets and pseudopotentials, as presented in Table 1.

In terms of effective core potential, and for the ground state $X^1\Sigma^+$, B_1 shows excellent agreement in the equilibrium bond length ($R_e = 2.024$ Å), closely matching the experimental value of 2.032 Å with only a 0.008 Å deviation. Case B_5, however, displays a much more important difference of 0.046 Å. At the same time, the vibrational constant ω_e from B_5 (1437.38 cm^{-1}) is slightly closer to the experimental value (1418 cm^{-1}) than that from B_1 (1447.28 cm^{-1}). For the excited state $(1)^3\Delta$, the ω_e and $\omega_e x_e$ values from B_1 align well with experimental values, whereas B_5 significantly underestimates this anharmonicity constant. Finally, for the $(1)^3\Pi$ state, B_1 yields excitation with an energy T_e, which is more consistent with available measurements.

These comparisons demonstrate that pseudopotential B_1 is more accurate and reliable for describing the spectroscopic properties of LaH, and it is therefore preferred in our study.

In terms of basis sets, B_3 yields a slightly improved vibrational constant ω_e (1468.69 cm^{-1}) compared to experiment (1418 cm^{-1}); however, it also leads to significantly higher deviations in $\omega_e x_e$. For the $(1)^3\Delta$ state, B_1 provides an excitation energy $T_e = 2179.37$ cm^{-1} and $R_e = 2.081$ Å, which are closer to experiment than those from B_4 or B_5, which overestimate R_e and show larger deviations in vibrational constants. Concerning the $(1)^3\Pi$ state, B_1 again delivers consistent performance, with $T_e = 4222.7$ cm^{-1} and $\omega_e = 1358.32$ cm^{-1}, reasonably close to the experimental values, while B_4 and B_5 significantly overestimate the excitation energy and distort vibrational constants.

Overall, B_1 exhibits the most balanced and accurate agreement across all three electronic states compared to experimental data. Therefore, the B_1 basis set (ECP28-MWB for La and aug-cc-pVQZ for H) is validated as the most suitable choice for describing the spectroscopic properties of LaH molecule.

Table 1 The spectroscopic constants of $X^1\Sigma^+$, $(1)^3\Delta$, and $(1)^3\Pi$ states of LaH molecule, without spin–orbit coupling using a benchmark of basis sets B_1–B_5, along with literature values, all compared with experimental data

States	Ref.	T_e (cm^{-1})	R_e (Å)	$\lvert\Delta R_e\rvert$ (Å)	ω_e (cm^{-1})	$\lvert\Delta\omega_e\rvert$ (cm^{-1})	$\omega_e x_e$ (cm^{-1})	$\lvert\Delta\omega_e x_e\rvert$ (cm^{-1})
$X^1\Sigma^+$	Exp.[24]	0.0	2.032		—		—	
	Exp.[25]	0.0	—		1418		15.6	
	This work$^{B}{}_1$	0.0	2.024	0.008	1447.28	29.28	15.43	0.17
	This work$^{B}{}_2$	0.0	2.024	0.008	1447.49	29.29	13.81	1.79
	This work$^{B}{}_3$	0.0	2.026	0.006	1468.69	50.69	28.79	13.19
	This work$^{B}{}_4$	0.0	2.078	0.046	1433.43	15.43	15.74	0.14
	This work$^{B}{}_5$	0.0	2.078	0.046	1437.38	19.38	15.45	0.15
	Theo.[29]	0.0	2.08	0.048	1433	15	—	—
	Theo.[30]	0.0	2.060	0.028	1429	11	20.93	5.33
	Theo.[31]	0.0	2.235	0.203	1353.26	64.74	—	—
	Theo.[32]	0.0	2.025	0.007	1439.77	21.77	15.242	0.358
$(1)^3\Delta$	Exp.[25]	—	—		1355		14.4	
	This work$^{B}{}_1$	2179.37	2.081		1347.34	7.66	15.22	0.82
	This work$^{B}{}_2$	1962.36	2.081		1371.59	16.59	15.89	1.49
	This work$^{B}{}_3$	2052.86	2.086		1357.44	2.44	11.02	3.38
	This work$^{B}{}_4$	2043.29	2.143		1338.96	16.04	14.49	0.09
	This work$^{B}{}_5$	2022.45	2.142		1335.94	19.06	11.03	3.37
	Theo.[29]	2805	2.13		1352	3.00	—	—
	Theo.[31]	3916	2.272		1314.98	40.02	—	—
	Theo.[32]	2232	2.082		1371.65	16.65	15.16	0.76
$(1)^3\Pi$	Exp.[25]	3732[a,b]	—		—		—	
	This work^{B_1}	4222.7	2.065		1358.32		18.39	
	This work^{B_2}	4222.74	2.064		1354.91		17.86	
	This work^{B_3}	4261.98	2.074		1343.06		18.05	
	This work^{B_4}	4764.40	2.145		1337.96		16.97	
	This work^{B_5}	4753.36	2.145		1314.65		17.75	
	Theo.[29]	5147	2.12		1341		—	
	Theo.[31]	3880	2.235		1341.37		—	
	Theo.[32]	4263	2.066		1359.20		18.65	

[a] Energy corresponding to ν_{00}. [b] Estimated energy of $^3\Lambda^{(\pm)}$ state determined by calculating the average of the spin–orbit components' energy. ^{B_1} This work using the ECP28MWB (s, p, d, f, g) basis set[37,38] for lanthanum and aug-cc-pVQZ (s, p, d, f)[36] for hydrogen. ^{B_2} This work using the ECP28MWB (s, p, d, f, g) basis set[37,38] for lanthanum and aug-cc-pV5Z (s, p, d, f)[39] for hydrogen. ^{B_3} This work using the ECP28MWB (s, p, d, f, g) basis set[37,38] for lanthanum and aug-cc-pVTZ (s, p, d)[39] for hydrogen. ^{B_4} This work using the ECP46MWB (s, p, d, f, g) basis set[35,40] for lanthanum and aug-cc-pV5Z (s, p, d, f)[39] for hydrogen. ^{B_5} This work using the ECP46MWB (s, p, d, f, g) basis set[35,40] for lanthanum and aug-cc-pVQZ (s, p, d, f)[36] for hydrogen. Theoretical work[31] used the ECP46MHF (s, p, d) basis set[35] for lanthanum and aug-cc-pVQZ (s, p, d, f)[36] for hydrogen.

3. *Ab initio* results

Our primary focus in this work is the study of the laser cooling of LaH, by considering transitions between the ground and low-lying excited states. The investigated potential energy curves for the three low-lying $\Lambda^{(\pm)}$ and $\Omega^{(\pm)}$ states: $X^1\Sigma^+$ ($X^1\Sigma_{0+}$), $(1)^3\Delta$ $\{(1)^3\Delta_1$, $(1)^3\Delta_2$, $(1)^3\Delta_3\}$, and $(1)^3\Pi$ $\{(1)^3\Pi_{0-}$, $(1)^3\Pi_{0+}$, $(1)^3\Pi_1$, $(1)^3\Pi_2\}$ are displayed as a function of internuclear separation in Fig. 1 and Fig. 2. The spin–orbit coupling splitting of the electronic states $(1)^3\Delta$ and $(1)^3\Pi$ of the molecule LaH is illustrated in Fig. 3. Due to the dominance of fine structure in the spectra of heavy molecules such as LaH, it is crucial to account for the spin–orbit interaction of lanthanum. This requirement is validated by the notably large splitting energies observed for the $^3\Delta$ state (approximately 448 cm^{-1} for $(1)^3\Delta_2$ – $(1)^3\Delta_1$) and $^3\Pi$ state (around 320 cm^{-1} for $(1)^3\Pi_2$ – $(1)^3\Pi_1$) electronic states, as illustrated in Fig. 2 and 3. These results highlight the significant influence of spin–orbit coupling on the electronic states of the LaH molecule. In addition, the transition dipole moment curves (TDMCs) of the allowed transitions $X^1\Sigma_{0+}$–$(1)^3\Pi_{0+}$ and

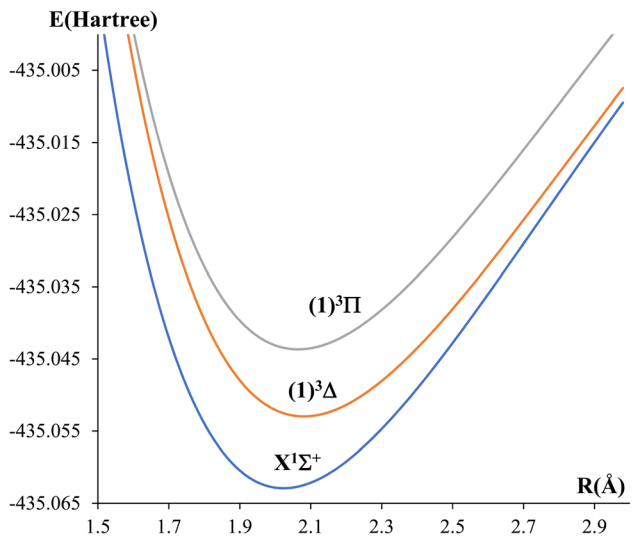

Fig. 1 The potential energy curves of the ground and first two low-lying excited states of the LaH molecule, in the $\Lambda^{(\pm)}$ representation.

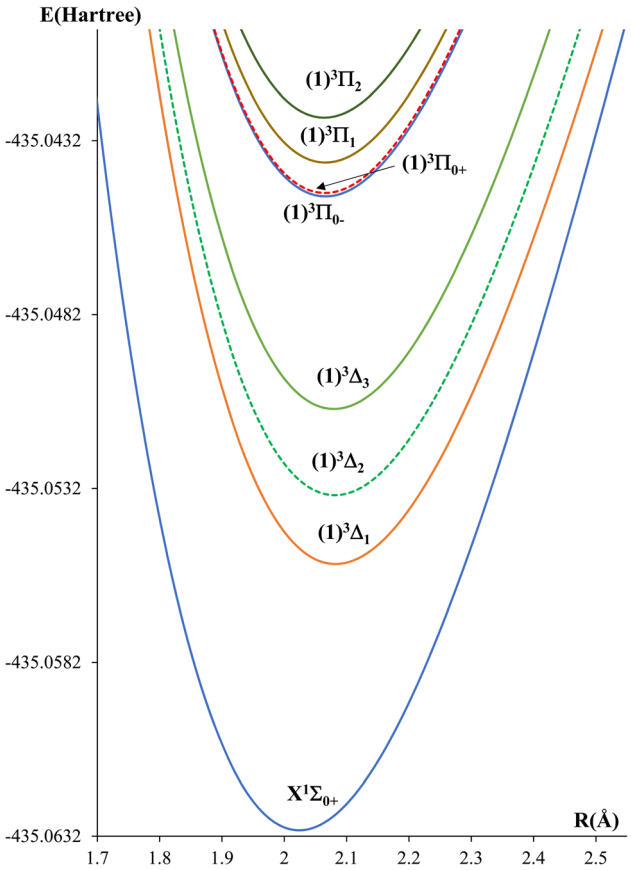

Fig. 2 The potential energy curves of the ground and first two low-lying excited states of the LaH molecule, in the $\Omega^{(\pm)}$ representation.

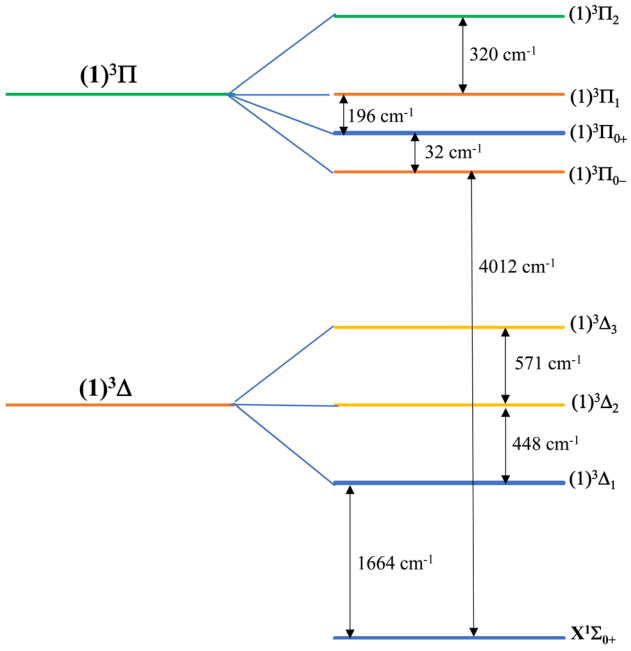

Fig. 3 Spin–orbit coupling splitting of the electronic states $(1)^3\Delta$ and $(1)^3\Pi$ of the molecule LaH.

$(1)^3\Pi_{0+}$–$(1)^3\Delta_1$ of the molecule LaH have been computed as a function of internuclear distance and displayed in Fig. 4.

The spectroscopic constants such as the equilibrium bond length R_e, the transition energy with respect to the ground state minimum T_e, the harmonic frequency ω_e, and the anharmonicity constant $\omega_e x_e$ of all the calculated $\Lambda^{(\pm)}$ (listed as (B_1) in Table 1) and $\Omega^{(\pm)}$ states are determined and listed in Table 2. As previously mentioned, the ground state has $^1\Sigma^+$ symmetry, and the first two low-lying excited states are $(1)^3\Delta$ and $(1)^3\Pi$. Their spectroscopic constants strongly agree with experimental data.[24,25] In the $\Lambda^{(\pm)}$ representation, the equilibrium internuclear distance R_e of the ground state exhibits a relative error of only 0.4% compared to the experimental value ($R_e = 2.032$ Å).[24] Similarly, the vibrational constants ω_e and $\omega_e x_e$ for $(1)^3\Delta$ state show relative errors of 0.6% and 5.7%, respectively, compared to experimental data.[25] The *ab initio* investigation of LaH conducted in 2014 [31] showed that the use of the large-core pseudopotential ECP46MHF[35] for lanthanum (La) with 10 valence electrons introduced considerable inaccuracies in the computed equilibrium bond lengths (R_e) of various electronic states, and the transition energies (T_e) for several predicted states were significantly overestimated. For instance, the ground state R_e deviated by approximately 9.4% from the experimental value.[24]

The transition energies (T_e) associated with the spin–orbit components of the $(1)^3\Delta$ and $(1)^3\Pi$ electronic states were not reported in the published experimental studies.[25] Instead, it only provided the energies corresponding to ν_{00}, *i.e.*, the T_0 values for these spin–orbit components. As a result, a direct comparison between our calculated T_e values and the experimental T_0 data is not feasible. For a meaningful comparison, we instead consider the spin–orbit splitting energies. However, the calculated splitting energy of the $(1)^3\Delta$ state is $\Delta\Omega_{1-2}$ (448 cm^{-1}), which is closer to the experimental value[25] ($\Delta\Omega_{1-2} = 387$ cm^{-1}). The calculated spin–orbit splitting for the $(1)^3\Pi$ state demonstrates a remarkably strong agreement with experimental observations reported in references.[25,27] The total splitting energy obtained from our calculations, $\Delta E_{Total} = 548$ cm^{-1}, aligns closely with the experimental value[25,27] of 506 cm^{-1}, differing by only ~7%. This level of agreement underscores the accuracy and reliability of the theoretical methods employed, particularly in capturing the fine-structure effects arising from spin–orbit coupling. Such consistency between theory and experiment validates the computational treatment of the $(1)^3\Pi$ state, which plays a key role in our analysis of electronic transitions and laser cooling feasibility.

4. Laser cooling study of the LaH molecule

Laser cooling is a technique that reduces the motion of atoms or molecules by repeatedly scattering photons through fast and controlled optical transitions.[43] Each photon scatter imparts a small, directional momentum change, effectively reducing the system's kinetic energy and entropy. Although both direct[44–47] methods (*e.g.*, buffer gas cooling, Stark deceleration) and

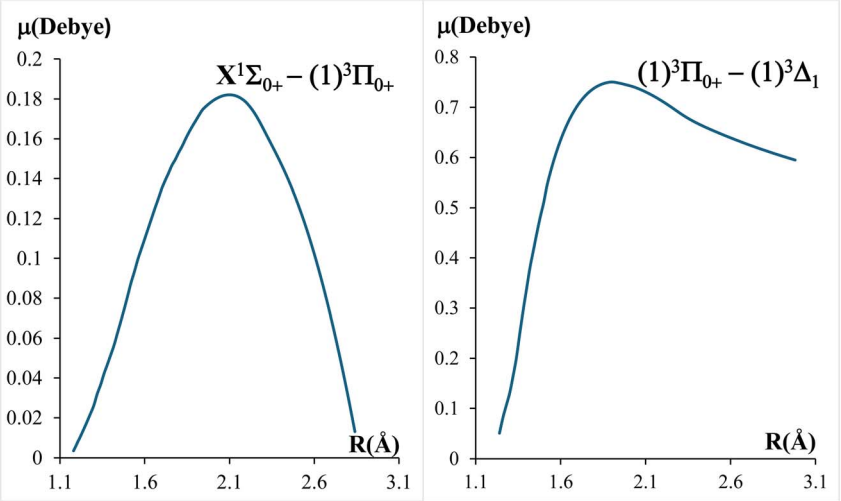

Fig. 4 Transition dipole moments of the transitions (a) $X^1\Sigma_{0+}$–$(1)^3\Pi_{0+}$ and (b) $(1)^3\Delta_1$–$(1)^3\Pi_{0+}$ of the molecule LaH.

indirect[48,49] methods (*e.g.*, photoassociation of cold atoms) can be used to achieve molecular cooling and trapping. Laser cooling has uniquely succeeded in reaching the sub-millikelvin range for various diatomic[50–53] and linear triatomic[54–56] species. Several criteria are to be followed when considering cooling transitions among vibronic levels in a diatomic molecule.

(i) A highly diagonal Franck–Condon array for the considered band system, which would ensure a low number of lasers that would be used to retain the closed-loop cycle of the molecule. One could usually recognize band systems with high Franck–Condon arrays when the equilibrium internuclear distance (R_e) among the considered electronic states is minimal.[57]

(ii) No intervening electronic state that would disturb the laser cooling cycle. One should make a distinction in this case between intervening and non-intervening electronic states. An intervening electronic state is usually an intermediate state situated between the excited state and the ground state, forming the cycling loop, and that intervenes with the transition band. This usually takes place if there is a high probability of transition between the upper-level electronic state and this intermediate state. A lower transition probability would render the intermediate state as non-intervening. Recent studies, however, have shown the possible involvement of intervening intermediate states in the cooling process.[58–60]

(iii) The transition radiative lifetime among the considered vibrational levels should be very short to ensure high photon scattering rates. Usually, the considered radiative lifetimes are in the range of ns-ms.[14,61,62]

The equilibrium positions difference ΔR_e between the ground state $X^1\Sigma_{0+}$ and the excited state $(1)^3\Pi_{0+}$ (about 0.0349 Å) of the molecule LaH is minimal. This encouraged the authors to consider a closed cycle formed from bands within these states. Fig. (5a) shows highly diagonal Franck–Condon arrays for the transitions $X^1\Sigma_{0+}$–$(1)^3\Pi_{0+}$ for the vibrational levels $0 \leq v \leq 5$, obtained using the Level 11 program,[63] thus fulfilling criteria (i).

Fig. 2 shows four intermediate states to the considered cycle: $(1)^3\Pi_{0-}$, $(1)^3\Delta_1$, $(1)^3\Delta_2$, and $(1)^3\Delta_3$. Transition among states $(1)^3\Pi_{0+}$ and $(1)^3\Pi_{0-}$ are not allowed due to the rule $0^+ \nrightarrow 0^-$ [64] in Hund's case-c. The transitions $(1)^3\Pi_{0+}$ – $(1)^3\Delta_2$ and $(1)^3\Pi_{0+}$ – $(1)^3\Delta_2$ are not allowed either, since transitions with $\Delta\Omega > 1$ are also forbidden[64] in Hund's case c. As a consequence, the laser cooling of the LaH molecule through the cycle made of the transitions $X^1\Sigma_{0+}$–$(1)^3\Pi_{0+}$ will necessitate investigating the intervening degree of the intermediate state $(1)^3\Delta_1$ only, as required through criteria (ii). The diagonality of the FCF for $(1)^3\Delta_1$–$(1)^3\Pi_{0+}$ is shown in Fig. (5b), showing a high transition probability to the first vibrational levels of the intermediate state.

Criteria (iiii) can be evaluated by considering the Transition Dipole Moment curves (TDMCs), *i.e.*, the transition dipole moment variation μ(R) in terms of the internuclear distance R among the involved electronic states. The TDMC for $X^1\Sigma_{0+}$–$(1)^3\Pi_{0+}$ and $(1)^3\Delta_1$–$(1)^3\Pi_{0+}$ transitions are given in Fig. 5, as obtained with the Molpro program.[33] The vibrational radiative lifetime $\tau_{vv'}$ can be calculated as the inverse of the Einstein coefficient $A_{vv'}$ $\left(\tau = \frac{1}{\sum_j A_{v''v}}\right)$.[65,66] The vibrational Einstein Coefficient among the transition $(1)^3\Delta_1$–$(1)^3\Pi_{0+}$ is calculated using the LEVEL 11 program according to the following formula:

$$A_{v'v} = (3.1361891)(10^{-7})(\Delta E)^3(\langle\psi_{v'}|\mu(r)|\psi_v\rangle)^2 \quad (1)$$

where $A_{vv'}$ has as units s^{-1}, ΔE is the emission frequency (in cm^{-1}) and $\mu(r)$ is the electronic transition dipole moment between the two considered electronic states (in Debye).[67] For transitions of the nature Σ – Π, such as $X^1\Sigma_{0+}$–$(1)^3\Pi_{0+}$, the transition dipole moment (TDM) is vertical, as calculated in terms of μ_x, μ_y, μ_z. In this case, the Einstein coefficient expressed in (1) has to be divided by two.[68]

Table 2 The spectroscopic constants of $X^1\Sigma^+$, $(1)^3\Delta$, and $(1)^3\Pi$ states with and without spin–orbit coupling of LaH

Spectroscopic constants in the $\Lambda^{(\pm)}$ representation

States	Ref.	T_e (cm^{-1})	$\Delta T_e/T_e$%	R_e (Å)	$\Delta R_e/R_e$%	ω_e (cm^{-1})	$\Delta\omega_e/\omega_e$%	$\omega_e x_e$ (cm^{-1})	$\Delta\omega_e x_e/\omega_e x_e$%
$X^1\Sigma^+$	This work	0.0		2.024	0.4	1447.28	—	15.43	—
	Exp.[24]	0.0		2.032	—	—	2.1	—	1.1
	Exp.[25]	0.0		—	2.7	1418	1.0	15.6	—
	Theo.[29]	0.0		2.08	1.7	1433	1.3	—	26.3
	Theo.[30]	0.0		2.060	9.4	1429	6.9	20.93	—
	Theo.[31]	0.0		2.235	0.0	1353.26	0.5	—	1.2
	Theo.[32]	0.0		2.025		1439.77		15.242	
$(1)^3\Delta$	This work	2179.37	—	2.081	—	1347.34	0.6	15.22	5.7
	Exp.[25]	—	22.3	—	2.3	1355	0.3	14.4	—
	Theo.[29]	2805	44.3	2.13	8.4	1352	2.5	—	—
	Theo.[31]	3916	2.4	2.272	0.0	1314.98	1.8	—	0.4
	Theo.[32]	2232		2.082		1371.65		15.16	
$(1)^3\Pi$	This work	4222.7	—	2.065	—	1358.32	—	18.39	—
	Exp.[25]	3732[a,b]	18.0	—	2.6	—	1.3	—	—
	Theo.[29]	5147	8.8	2.12	7.6	1341	1.3	—	—
	Theo.[31]	3880	0.9	2.235	0.0	1341.37	0.1	—	1.4
	Theo.[32]	4263		2.066		1359.20		18.65	

Spectroscopic constants in the $\Omega^{(\pm)}$ representation

States	Ref.	T_e (cm^{-1})	$\Delta T_e/T_e$%	R_e (Å)	$\Delta R_e/R_e$%	ω_e (cm^{-1})	$\Delta\omega_e/\omega_e$%	$\omega_e x_e$ (cm^{-1})	$\Delta\omega_e x_e/\omega_e x_e$%
$X^1\Sigma^+{}_0{}^+$	This work	0.0		2.027	—	1443.63	1.8	14.56	6.7
	Exp.[25]	0.0		—	0.2	1418	—	15.6	—
	Theo.[29]	0.0		2.0319	0.0	—	0.1	—	8.5
	Theo.[32]	0.0		2.027		1444.66		15.904	
$(1)^3\Delta_1$	This work	1664.4	—	2.080	1.4	1359.66	—	13.67	—
	Exp.[23]	—	—	2.1102	—	—	0.3	—	5.1
	Exp.[25]	1259.5[a]	—	—	0.9	1355	—	14.4	—
	Theo.[29]	—	0.0	2.099	0.2	—	0.3	—	4.6
	Theo.[32]	1665		2.085		1363.659		14.331	
$(1)^3\Delta_2$	This work	2112.1	—	2.078	0.8	1363.87	—	14.79	—
	Exp.[23]	—	—	2.0938	—	—	—	—	—
	Exp.[25]	1646[a]	—	—	0.2	—	—	—	—
	Theo.[29]	—	0.1	2.083	0.3	—	0.2	—	2.4
	Theo.[32]	2111		2.084		1366.582		15.15	
$(1)^3\Delta_3$	This work	2682.8	—	2.085		1371.49		17.81	—
	Exp.[23]	—	—	2.0925	0.4	—	—	—	—
	Theo.[29]	—	0.0	2.081	0.2	—	0.1	—	0.8
	Theo.[32]	2684		2.082	0.1	1373.275		17.960	
$(1)^3\Pi_{0-}$	This work	4011.9	—	2.0637	—	1356.63	—	15.656	—
	Exp.[25]	3542[a]	0.1	—	0.2	—	0.3	—	2.0
	Theo.[32]	4014		2.068		1352.946		15.977	
$(1)^3\Pi_{0+}$	This work	4043.9	—	2.0619	—	1361.47	—	17.899	—
	Exp.[25]	3586[a]	0.1	—	0.2	—	0.2	—	2.4
	Theo.[32]	4047		2.067		1358.629		18.345	
$(1)^3\Pi_1$	This work	4239.7	—	2.0646	—	1352.34	—	16.478	—
	Exp.[25]	3754[a]	0.0	—	0.1	—	0.1	—	1.1
	Theo.[32]	4241		2.067		1353.606		16.669	
$(1)^3\Pi_2$	This work	4559.7	—	2.0639	—	1369.78	—	15.975	—
	Exp.[27]	4048[a]	0.1	—	0.1	—	0.1	—	3.6
	Theo.[32]	4557		2.065		1367.963		16.579	

[a] Energy corresponding to ν_{00}. [b] Estimated energy of $^3\Lambda^{(\pm)}$ state determined by calculating the average of the spin–orbit components' energy.

The vibrational branching loss ratio measures how much an intermediate state affects a laser cooling cycle between two other states. In our study, we have to examine how the intermediate state $(1)^3\Delta_1$ influences the cycle between the $X^1\Sigma_{0+}$ and $(1)^3\Pi_{0+}$ states. The vibrational branching loss ratio to this state is approximately equal to:

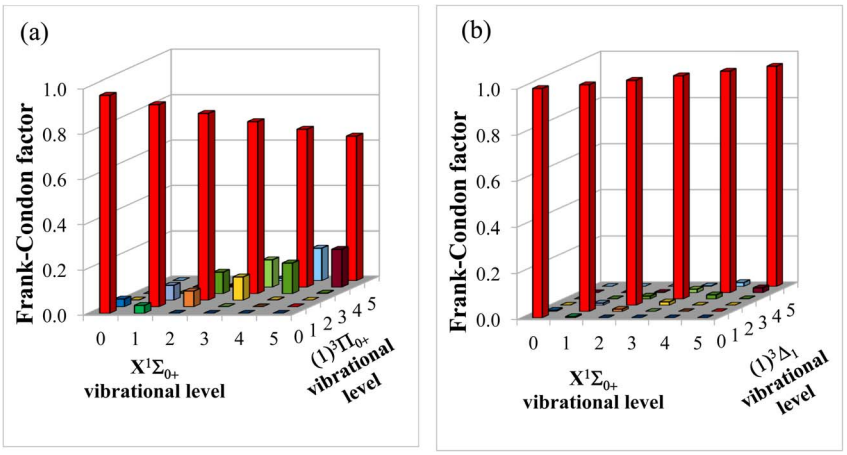

Fig. 5 The Frank–Condon factor of the transitions $X^1\Sigma_{0+}$–$(1)^3\Pi_0$ and $(1)^3\Delta_1$–$(1)^3\Pi_0$ of the molecule LaH.

$$\eta = \frac{A_{0\nu'}\left((1)^3\Pi_{0+} \rightarrow (1)^3\Delta_1\right)}{A_{0\nu'}\left((1)^3\Pi_{0+} \rightarrow (X)^3\Sigma_{0+}\right)} \cong 7$$

Given the high degree of interference of the intermediate state with the cycling loop, the laser cooling analysis will be one to include the intermediate state, as done previously in the literature.[69,70] The vibrational branching ratio, which represents the percentage of transition probability between two vibrational levels, is obtained by using the formula:[71]

$$R_{\nu'\nu} = \frac{A_{\nu'\nu}}{\sum A_{\nu'\nu}} \quad (2)$$

Since we are studying the laser cooling between the two electronic states $(1)^3\Pi_{0+}$ and $X^1\Sigma_{0+}$ with the intermediate state $(1)^3\Delta_1$, the values of the vibrational branching ratio $R_{\nu''\nu}$ and $R_{\nu''\nu'}$ for the first five vibrational levels are given by:[72]

$$(1)^3\Pi_{0+} - X^1\Sigma_{0+} \rightarrow R_{\nu''\nu} = \frac{A_{\nu''\nu}}{\sum A_{\nu''\nu'} + \sum A_{\nu'\nu}} \quad (3.1)$$

$$(1)^3\Pi_{0+} - (1)^3\Delta_1 \rightarrow R_{\nu''\nu'} = \frac{A_{\nu''\nu'}}{\sum A_{\nu''\nu'} + \sum A_{\nu'\nu}} \quad (3.2)$$

where $A_{\nu''\nu}$ and $A_{\nu''\nu'}$ are the Einstein coefficients for the transitions $(1)^3\Pi_{0+}$–$X^1\Sigma_{0+}$ and $(1)^3\Pi_{0+}$–$(1)^3\Delta_1$, respectively. The corresponding calculated values of these Einstein coefficients and

Table 3 The radiative lifetimes τ, and the vibrational branching ratio of the vibrational transitions. Between the electronic states $(1)^3\Pi_{0+} - X^1\Sigma_{0+}$ and $(1)^3\Pi_{0+} - (1)^3\Delta_1$ of the molecule LaH

		$\nu''\ ((1)^3\Pi_{0+}) = 0$	1	2	3	4	5
$\nu\ (({}^1X_{0+})) = 0$	$A_{\nu\nu''}$	2458.937631	130.9866596	2.52485×10^{-5}	1.017740631	0.185340271	0.02356491
	$R_{\nu\nu''}$	0.123427154	0.01235997	2.52701×10^{-9}	2.52701×10^{-9}	2.1245×10^{-5}	3.29397×10^{-5}
1	$A_{\nu''}$	54.13476602	1988.819523	269.2849008	0.732617602	3.268505736	0.990 576 903
	$R_{\nu\nu''}$	0.002717312	0.187666051	0.026951574	8.13052×10^{-5}	0.000374658	0.001384656
2	$A_{\nu\nu''}$	0.212860911	84.56872455	1574.649772	392.4625508	5.437394721	4.106859785
	$R_{\nu\nu''}$	1.06846×10^{-5}	0.007979949	0.15759996	0.043555105	0.000623271	0.005740684
3	$A_{\nu\nu''}$	0.009726067	0.804036255	99.6551288	1230.988993	502.8191021	14.80275134
	$R_{\nu\nu''}$	4.88203×10^{-7}	7.58693×10^{-5}	0.009974056	0.136613938	0.057636543	0.020691701
4	$A_{\nu\nu''}$	0.000172085	0.019056646	1.710011321	101.2045812	927.9466442	601.3369858
	$R_{\nu\nu''}$	8.63788×10^{-9}	1.7982×10^{-6}	0.000171148	0.011231584	0.106367552	0.840565695
$\nu'\ ((1)^3\Delta_1) = 0$	$A_{\nu'\nu''}$	17353.11041	56.71484895	0.36948472	6.17829E-10	6.17829E-10	0.000120469
	$R_{\nu'\nu''}$	0.871044876	0.005351643	3.69801×10^{-5}	6.8566×10^{-14}	7.08197×10^{-14}	1.68395×10^{-7}
1	$A_{\nu'\nu''}$	43.77651799	8225.202174	52.13234864	0.000400248	0.000400248	2.85186×10^{-6}
	$R_{\nu'\nu''}$	0.002197376	0.776134381	0.005217704	4.44191×10^{-8}	4.58792×10^{-8}	3.98641×10^{-9}
2	$A_{\nu'\nu''}$	10.64881134	78.79191542	7837.876719	1.211771658	1.211771658	0.001 576 422
	$R_{\nu'\nu''}$	0.00053452	0.007434846	0.784459554	0.000134481	0.000138902	2.20357×10^{-6}
3	$A_{\nu'\nu''}$	1.304985207	26.12163032	111.8377067	82.58291984	82.58291984	1.955219988
	$R_{\nu'\nu''}$	6.55041×10^{-5}	0.002464851	0.011193358	0.009164971	0.009466216	0.002733061
4	$A_{\nu'\nu''}$	0.04137685	5.623563619	43.91900286	7200.511483	7200.511483	92.1779253
	$R_{\nu'\nu''}$	2.07692×10^{-6}	0.000530642	0.004395665	0.799105624	0.825371568	0.128848888
$\Sigma A_{\nu\nu''}$		19922.17726	10597.65213	9991.4351	9010.713057	8723.963561	715.3955837
$\tau = 1/\Sigma A_{\nu\nu'}$		5.01953×10^{-5}	9.43605×10^{-5}	0.000100086	0.000110979	0.000114627	0.001397828
τ (μs)		50.2	94.4	100.1	111.0	114.6	1397.8

the vibrational branching ratio are given in Table 3, along with the value of the radiative lifetime, which is within the experimental conditions to realize the laser cooling of the molecule LaH. The experimental parameters needed to realize laser cooling are[73]

$$V = \frac{hN}{m\lambda_{00}} \tag{4.1}$$

$$T_{\mathrm{ini}} = \frac{mV^2}{2k_{\mathrm{B}}} \tag{4.2}$$

$$A_{\max} = \frac{hN_{\mathrm{e}}}{N_{\mathrm{tot}}m\lambda_{00}\tau} \tag{4.3}$$

$$L = \frac{k_{\mathrm{B}}T_{\mathrm{ini}}}{ma_{\max}} \tag{4.4}$$

where h and k_{B} are, respectively, the Planck and Boltzmann constants, m is the mass of the molecule, and V, $a_{\max}$, and L are the speed, the maximum acceleration, and the slowing distance, respectively. In the main cycling transition, N_{e} is the number of the excited states, while N_{tot} is the number of the excited states connected to the ground state plus N_{e}.

The laser cooling scheme for the molecule LaH for the main transition $(1)^3\Pi_{0+}$–$X^1\Sigma_{0+}$ with the intermediate state $(1)^3\Delta_1$ is given in Fig. 6. The driving and the repumping lasers (of wavelengths $\lambda_{0''0} = 1258.8$ nm, $\lambda_{0''2} = 1927.5$ nm) are given in solid red lines for the transition $(1)^3\Pi_{0+}$–$X^1\Sigma_{0+}$ and in solid green lines (of wavelengths $\lambda_{0''0'} = 2147.3$ nm, $\lambda_{0''1'} = 1676.1$ nm) for the transition $(1)^3\Pi_{0+}$–$(1)^3\Delta_1$. These four suggested lasers are in the near-infrared region, a region of the spectrum for which commercial lasers are already available in the market. The spontaneous decays are represented in blue dotted lines for the transition $(1)^3\Pi_{0+}$–$X^1\Sigma_{0+}$ and in purple dotted lines for the transition $(1)^3\Pi_{0+}$–$(1)^3\Delta_1$. The values of the FCF ($f_{v''v}$ and $f_{v''v'}$) and the vibrational branching ratios $R_{v''v}$ and $R'_{v''}$ are specified for the vibrational levels in the laser cooling scheme. The loss to the vibrational level $v = 2$ is negligible ($R_{0''2} = 1.06846 \times 10^{-5}$), so that the corresponding vibrational level is not considered in the laser cooling scheme.

The number of cycles (N) for photon absorption/emission for the vibrational levels is reciprocal to the total loss:

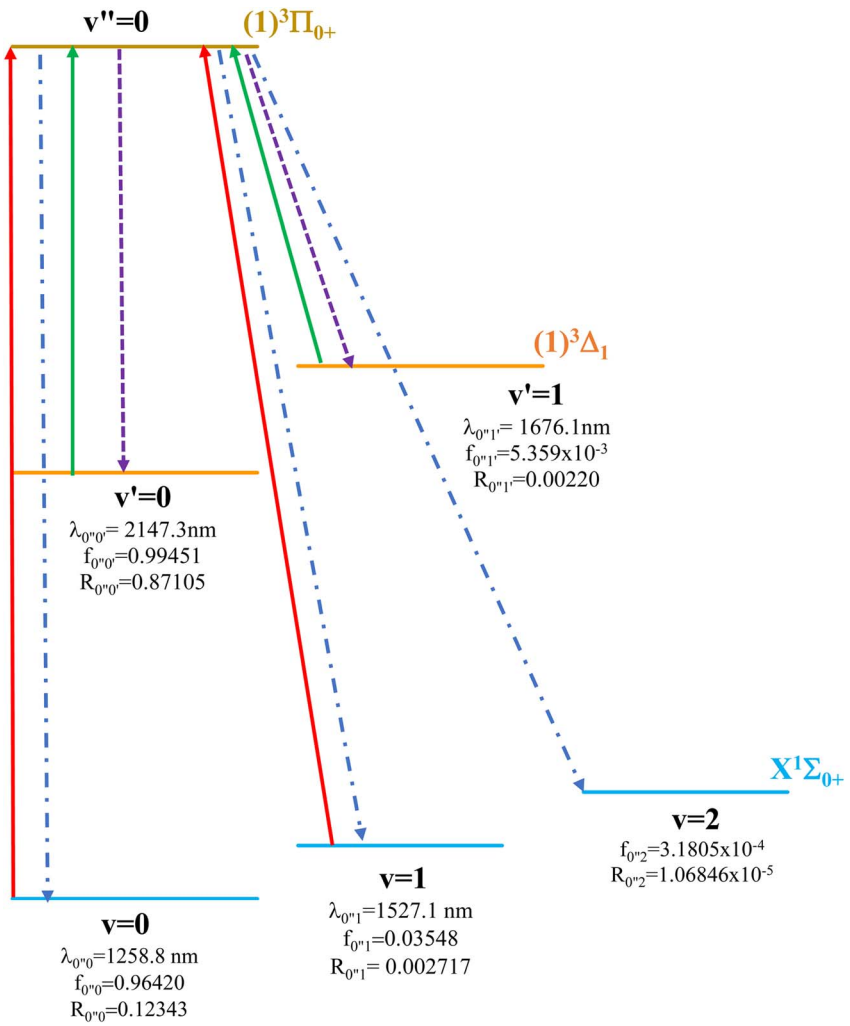

Fig. 6 Laser cooling scheme of transitions $X^1\Sigma_{0+}$–$(1)^3\Pi_0$ and $(1)^3\Delta_1$–$(1)^3\Pi_0$ of the molecule LaH.

$$N = \frac{1}{1 - \left[\left(R_{0''0} + R_{0''1}\right) + \left(R_{0''0'} + R_{0''1'}\right)\right]} = 1631 \quad (5)$$

The values of the corresponding experimental parameters are $L = 6.05$ m, V = 3.73 m s^{-1}, $T_{ini} = 0.117$ K, $N_e/N_{tot} = 1/5$, and $a_{max} = 1.15$ m s^{-2}. For this cooling scheme, the temperature that can be reached during the process is given by the Doppler limit temperature T_D and the recoil temperature T_r:[71]

$$T_D = h/(4 \times \pi \times \tau \times k_B) = 9.6 \text{ nK and}$$
$$T_r = h^2/(m \times \lambda^2_{00} \times k_B) = 88.1 \text{ nK}, \quad (6)$$

5. Conclusion

A theoretical *ab initio* calculation has been done based on a complete active space self-consistent field (CASSCF)/(MRCI + Q) with Davidson correction in the $\Lambda^{(\pm)}$ and $\Omega^{(\pm)}$ representations. The calculation of the adiabatic potential energy curves, the spectroscopic constants, the FCFs, and the radiative lifetime for the transition $X^1\Sigma_{0+}$–$(1)^3\Pi_{0+}$ shows the candidacy of the LaH molecule for direct laser cooling. The calculation of the FCF and the radiative lifetime for the transition $(1)^3\Delta_1$–$(1)^3\Pi_{0+}$ shows that the presence of the intermediate state $(1)^3\Delta$ between $X^1\Sigma_{0+}$ and $(1)^3\Pi_{0+}$ cannot be ignored. Therefore, a total vibrational branching ratio is calculated, leading to a total radiative lifetime ($\tau = 50.2$ μs). Experimental parameters such as the Doppler and recoil temperatures, the slowing distance, and the number of cycles (N) for photon absorption/emission are proposed. A laser cooling scheme is presented for the transition $X^1\Sigma_{0+}$–$(1)^3\Pi_{0+}$ with the intermediate state $(1)^3\Delta_1$. These results open the way for direct laser cooling of the molecule LaH.

Conflicts of interest

The authors declare no competing interests.

Data availability

All data generated or analysed during this study are included in this published article.

Acknowledgements

This publication is based upon work supported by the Khalifa University of Science and Technology under Award No. RIG-2024-053 and the Abu-Dhabi Department of Education and Knowledge, under award number AARE20-031. Al MESBAR High Power Computer was used for the completion of this work.

References

1 R. Blatt, P. Gill and R. C. Thompson, Current Perspectives on the Physics of Trapped Ions, *J. Mod. Opt.*, 1992, **39**(2), 193–220, DOI: 10.1080/09500349214550221.
2 S. A. Diddams, Th. Udem, J. C. Bergquist, E. A. Curtis, R. E. Drullinger, L. Hollberg, W. M. Itano, W. D. Lee, C. W. Oates, K. R. Vogel and D. J. Wineland, An Optical Clock Based on a Single Trapped 199Hg+ Ion, *Science*, 2001, **293**(5531), 825–828, DOI: 10.1126/science.1061171.
3 K. Góral, L. Santos and M. Lewenstein, Quantum Phases of Dipolar Bosons in Optical Lattices, *Phys. Rev. Lett.*, 2002, **88**(17), 170406, DOI: 10.1103/PhysRevLett.88.170406.
4 R. Barnett, D. Petrov, M. Lukin and E. Demler, Quantum Magnetism with Multicomponent Dipolar Molecules in an Optical Lattice, *Phys. Rev. Lett.*, 2006, **96**(19), 190401, DOI: 10.1103/PhysRevLett.96.190401.
5 A. Micheli, G. K. Brennen and P. Zoller, A toolbox for lattice-spin models with polar molecules, *Nat. Phys.*, 2006, **2**(5), 341–347, DOI: 10.1038/nphys287.
6 R. V. Krems, Cold controlled chemistry, *Phys. Chem. Chem. Phys.*, 2008, **10**(28), 4079–4092, DOI: 10.1039/B802322K.
7 Y. Gao and T. Gao, Laser cooling of the alkaline-earth-metal monohydrides: Insights from an *ab initio* theory study, *Phys. Rev. A*, 2014, **90**(5), 052506, DOI: 10.1103/PhysRevA.90.052506.
8 C. Li, Y. Li, Z. Ji, X. Qiu, Y. Lai, J. Wei, Y. Zhao, L. Deng, Y. Chen and J. Liu, Candidates for direct laser cooling of diatomic molecules with the simplest $^1\Sigma$ – $^1\Sigma$ electronic system, *Phys. Rev. A*, 2018, **97**(6), 062501, DOI: 10.1103/PhysRevA.97.062501.
9 M.-S. Xu, C.-L. Yang, M.-S. Wang and X.-G. Ma, Theoretical study on the low-lying excited electronic states and laser cooling feasibility of CuH molecule, *Spectrochim. Acta. A. Mol. Biomol. Spectrosc.*, 2019, **212**, 55–60, DOI: 10.1016/j.saa.2018.12.038.
10 M.-S. Xu, C.-L. Yang, M.-S. Wang, X.-G. Ma and W.-W. Liu, Theoretical study on the low-lying electronic excited states and laser cooling feasibility of AuH molecule, *J. Quant. Spectrosc. Radiat. Transf.*, 2020, **242**, 106770, DOI: 10.1016/j.jqsrt.2019.106770.
11 N. Wells and I. C. Lane, Prospects for ultracold carbonvia charge exchange reactions and laser cooled carbides, *Phys. Chem. Chem. Phys.*, 2011, **13**(42), 19036–19051, DOI: 10.1039/C1CP21304K.
12 N. Wells and I. C. Lane, Electronic states and spin-forbidden cooling transitions of AlH and AlF, *Phys. Chem. Chem. Phys.*, 2011, **13**(42), 19018–19025, DOI: 10.1039/C1CP21313J.
13 J. H. V. Nguyen, C. R. Viteri, E. G. Hohenstein, C. D. Sherrill, K. R. Brown and B. Odom, Challenges of laser-cooling molecular ions, *New J. Phys.*, 2011, **13**(6), 063023, DOI: 10.1088/1367-2630/13/6/063023.
14 A. El K. Nariman, *et al.*, Electronic Structure with Spin-Orbit Coupling Effect of HfH Molecule for Laser Cooling Investigations, *Spectrochim. Acta, Part A*, 2024, **314**, 124106, DOI: 10.1016/j.saa.2024.124106.
15 F. Furche and J. P. Perdew, The performance of semilocal and hybrid density functionals in 3d transition-metal chemistry, *J. Chem. Phys.*, 2006, **124**(4), 044103, DOI: 10.1063/1.2162161.

16 J. G. Harrison, Density functional calculations for atoms in the first transition series, *J. Chem. Phys.*, 1983, **79**(5), 2265–2269, DOI: 10.1063/1.446076.
17 K. P. Jensen, B. O. Roos and U. Ryde, Performance of density functionals for first row transition metal systems, *J. Chem. Phys.*, 2007, **126**(1), 014103, DOI: 10.1063/1.2406071.
18 J. F. Harrison, Electronic Structure of Diatomic Molecules Composed of a First-Row Transition Metal and Main-Group Element (H–F), *Chem. Rev.*, 2000, **100**(2), 679–716, DOI: 10.1021/cr980411m.
19 A. J. Sauval, Predicted presence and tentative identification of new molecules in the pure S star R CYG, *Astron. Astrophys.*, 1978, **62**, 295–298.
20 J. A. M. Simoes and J. L. Beauchamp, *Transition metal-hydrogen and metal-carbon bond strengths: the keys to catalysis*, ACS Publications, 2023, DOI: 10.1021/cr00102a004.
21 F. A. Cotton and G. Wilkinson, *Advanced Inorganic Chemistry, A Comprehensive Text*, 5th edn., Wiley, New York, 1988.
22 E. R. Meyer, J. L. Bohn and M. P. Deskevich, Candidate molecular ions for an electron electric dipole moment experiment, *Phys. Rev. A*, 2006, **73**, 062108, DOI: 10.1103/PhysRevA.73.062108.
23 R. B. Bernard, *Can. J. Phys.*, 1976, **54**(14), 1509.
24 R. S. Ram and P. F. Bernath, *J. Chem. Phys.*, 1996, **104**(17), 6444.
25 S. Mukund and S. Yarlagadda, Energy linkage between the singlet and triplet manifolds in LaH, and observation of new low-energy states, *J. Chem. Phys.*, 2012, **137**, 234309.
26 S. Yarlagadda, S. Mukund and S. G. Nakhate, Jet-cooled laser-induced fluorescence spectroscopy of LaH: Observation of new excited electronic states, *Chem. Phys. Lett.*, 2012, **537**, 1.
27 S. Yarlagadda, S. Mukund, S. Bhattacharyya and S. G. Nakhate, *J. Mol. Spectrosc.*, 2013, **289**, 1.
28 S. Yarlagadda, S. Mukund, S. Bhattacharyya and S. G. Nakhate, *J. Quant. Spectrosc. Radiat. Transfer*, 2014, **145**, 17.
29 K. D. Das and K. Balasubramanian, *Chem. Phys. Lett.*, 1990, **172**, 372.
30 S. Koseki, Y. Ishihara, D. G. Fedorov, H. Umeda, *et al.*, *J. Phys. Chem. A*, 2004, **108**(21), 4707.
31 S. Mahmoud and M. Korek, Theoretical calculation of the low-lying electronic states of the LaH molecule, *Can. J. Chem.*, 2014, **92**(9), 855–861, DOI: 10.1139/cjc-2014-0057.
32 J. Assaf, R. Assaf and E. C. M. Nascimento, New insight into the spectroscopy of LaH by *ab initio* methods, *Comput. Theor. Chem.*, 2021, **1203**, 113363, DOI: 10.1016/j.comptc.2021.113363.
33 H.-J. Werner, *et al.*, The molpro quantum chemistry package, *J. Chem. Phys.*, 2020, **152**(14), 144107, DOI: 10.1063/5.0005081.
34 A.-R. Allouche, Gabedit—a graphical user interface for computational chemistry softwares, *J. Comput. Chem.*, 2011, **32**(1), 174–182, DOI: 10.1002/jcc.21600.
35 M. Dolg, H. Stoll, A. Savin and H. Preuss, *Theor. Chim. Acta*, 1989, **75**, 173.
36 B. P. Pritchard, D. Altarawy, B. Didier, T. D. Gibson and T. L. Windus, A New Basis Set Exchange: An Open, Up-to-date Resource for the Molecular Sciences Community, *J. Chem. Inf. Model.*, 2019, **59**(11), 4814–4820, DOI: 10.1021/acs.jcim.9b00725.
37 X. Cao and M. Dolg, Valence basis sets for relativistic energy-consistent small-core lanthanide pseudopotentials, *J. Chem. Phys.*, 2001, **115**, 7348, DOI: 10.1063/1.1406535.
38 X. Cao and M. Dolg, Segmented contraction scheme for small-core lanthanide pseudopotential basis sets, *J. Molec. Struct. (Theochem)*, 2002, **581**, 139, DOI: 10.1016/S0166-1280(01)00751-5.
39 R. A. Kendall, T. H. Dunning and R. J. Harrison, Electron affinities of the first-row atoms revisited. Systematic basis sets and wave functions, *J. Chem. Phys.*, 1992, **96**, 6796–6806.
40 M. Dolg, H. Stoll and H. Preuss, *Theor. Chim. Acta*, 1993, **85**, 441.
41 J. Yang and M. Dolg, *Theor. Chem. Acc.*, 2005, **113**, 212.
42 A. Weigand, X. Cao, J. Yang and M. Dolg, *Theor. Chem. Acc.*, 2009, **126**, 117.
43 D. Mitra, N. B. Vilas, C. Hallas, L. Anderegg, B. L. Augenbraun, L. Baum, C. Miller, S. Raval and J. M. Doyle, Direct laser cooling of a symmetric top molecule, *Science*, 2020, **369**, 1366–1369.
44 M. Lemeshko, R. V. Krems, J. M. Doyle and S. Kais, Manipulation of molecules with electromagnetic fields, *Mol. Phys.*, 2013, **111**, 1648–1682.
45 A. Prehn, M. Ibrügger, R. Glöckner, G. Rempe and M. Zeppenfeld, Optoelectrical Cooling of Polar Molecules to Submillikelvin Temperatures, *Phys. Rev. Lett.*, 2016, **116**, 063005.
46 X. Wu, T. Gantner, M. Koller, M. Zeppenfeld, S. Chervenkov and G. Rempe, A cryofuge for cold-collision experiments with slow polar molecules, *Science*, 2017, **358**, 645–648.
47 Y. Liu, M. Vashishta, P. Djuricanin, S. Zhou, W. Zhong, T. Mittertreiner, D. Carty and T. Momose, Magnetic Trapping of Cold Methyl Radicals, *Phys. Rev. Lett.*, 2017, **118**, 093201.
48 K.-K. Ni, S. Ospelkaus, M. H. G. de Miranda, A. Pe'er, B. Neyenhuis, J. J. Zirbel, S. Kotochigova, P. S. Julienne, D. S. Jin and J. Ye, A high phase-space-density gas of polar molecules, *Science*, 2008, **322**, 231–235.
49 L. De Marco, G. Valtolina, K. Matsuda, W. G. Tobias, J. P. Covey and J. Ye, A degenerate Fermi gas of polar molecules, *Science*, 2019, **363**, 853–856.
50 E. S. Shuman, J. F. Barry and D. Demille, Laser cooling of a diatomic molecule, *Nature*, 2010, **467**, 820–823.
51 S. Truppe, H. J. Williams, M. Hambach, L. Caldwell, N. J. Fitch, E. A. Hinds, B. E. Sauer and M. R. Tarbutt, Molecules cooled below the Doppler limit, *Nat. Phys.*, 2017, **13**, 1173–1176.
52 L. Anderegg, B. L. Augenbraun, E. Chae, B. Hemmerling, N. R. Hutzler, A. Ravi, A. Collopy, J. Ye, W. Ketterle and J. M. Doyle, Radio Frequency Magneto-Optical Trapping of CaF with High Density, *Phys. Rev. Lett.*, 2017, **119**, 103201.
53 A. L. Collopy, S. Ding, Y. Wu, I. A. Finneran, L. Anderegg, B. L. Augenbraun, J. M. Doyle and J. Ye, 3D Magneto-

Optical Trap of Yttrium Monoxide, *Phys. Rev. Lett.*, 2018, **121**, 213201.

54 I. Kozyryev, L. Baum, K. Matsuda, B. L. Augenbraun, L. Anderegg, A. P. Sedlack and J. M. Doyle, Sisyphus Laser Cooling of a Polyatomic Molecule, *Phys. Rev. Lett.*, 2017, **118**, 173201.

55 B. L. Augenbraun, Z. D. Lasner, A. Frenett, H. Sawaoka, C. Miller, T. C. Steimle and J. M. Doyle, Laser-cooled polyatomic molecules for improved electron electric dipole moment searches, *New J. Phys.*, 2020, **22**, 022003.

56 L. Baum, N. B. Vilas, C. Hallas, B. L. Augenbraun, S. Raval, D. Mitra and J. M. Doyle, 1D Magneto-Optical Trap of Polyatomic Molecules, *Phys. Rev. Lett.*, 2020, **124**, 133201.

57 M. D. Di Rosa, Laser-Cooling Molecules: Concept, Candidates, and Supporting Hyperfine-Resolved Measurements of Rotational Lines in the AX (0, 0) Band of CaH, *Eur. Phys. J. D*, 2004, **31**, 395–402.

58 N. El-Kork, A. AlMasri Alwan, N. Abu El Kher, J. Assaf, T. Ayari, E. Alhseinat and M. Korek, Laser cooling with intermediate state of spin-orbit coupling of LuF molecule, *Sci. Rep.*, 2023, **13**(1), 7087, DOI: **10.1038/s41598-023-32439-1**.

59 A. Moussa, *et al.*, Laser Cooling with an Intermediate State and Electronic Structure Studies of the Molecules CaCs and CaNa, *ACS Omega*, 2022, **7**(22), 18577–18596, DOI: **10.1021/acsomega.2c01224**.

60 Y. Xiang *et al.*, Laser-Cooling with an Intermediate Electronic State: Theoretical Prediction on Bismuth Hydride, *J. Chem. Phys.* **150**, no. 22 (2019), **https://pubs.aip.org/aip/jcp/article/150/22/224305/197640**.

61 A. Madi, *et al.*, Theoretical Electronic Structure with Spin–Orbit Coupling Effect of the Molecules SrAt and BaAt for Laser Cooling Studies, *Sci. Rep.*, 2024, **14**(1), 6289.

62 F. Rabah *et al.*, Theoretical Spin–Orbit Laser Cooling for AlZn Molecule, *J. Chem. Phys.* **161**, no. 15 (2024), **https://pubs.aip.org/aip/jcp/article/161/15/154305/3317272**.

63 R. Le Roy, LEVEL: A Computer Program for Solving the Radial Schrödinger Equation for Bound and Quasibound Levels, *JQSRT*, 2017, **186**, 167–178.

64 G. Herzberg, *Molecular spectra and molecular structure. I Diatomic molecules*, ACS Publications. 2023, DOI: **10.1021/j150403a025**.

65 Y. Gao and T. Gao, Laser Cooling of BH and GaF: Insights from an *Ab Initio* Study, *Phys. Chem. Chem. Phys.*, 2015, **17**(16), 10830–10837.

66 I. Zeid, *et al.*, A Theoretical Electronic Structure with a Feasibility Study of Laser Cooling of LaNa Molecules with a Spin Orbit Effect, *Phys. Chem. Chem. Phys.*, 2022, **24**(13), 7862–7873.

67 S.-Y. Kang, *et al.*, Ab Initio Study of Laser Cooling of AlF+ and AlCl+ Molecular Ions, *J. Phys. B: At., Mol. Opt. Phys.*, 2017, **50**(10), 105103.

68 P. F. Bernath, *Spectra of Atoms and Molecules*, third edn, Oxford University press 2016.

69 A. Moussa, *et al.*, Laser Cooling with an Intermediate State and Electronic Structure Studies of the Molecules CaCs and CaNa, *ACS Omega*, 2022, **7**(22), 18577–18596, DOI: **10.1021/acsomega.2c01224**.

70 Y. Xiang *et al.*, Laser-Cooling with an Intermediate Electronic State: Theoretical Prediction on Bismuth Hydride, *J. Chem. Phys.* **150**, no. 22 (2019), **https://pubs.aip.org/aip/jcp/article/150/22/224305/197640**.

71 R. Li, X. Yuan, G. Liang, Y. Wu, J. Wang and B. Yan, Laser Cooling of the SiO+ Molecular Ion: A Theoretical Contribution, *Chem. Phys.*, 2019, **525**, 110412.

72 Y. Xiang, H.-J. Guo, Yu-M. Wang, J.-L. Xue, H.-F. Xu and B. Yan, *J. Chem. Phys.*, 2019, **150**, 224305, DOI: **10.1063/1.5094367**.

73 J. F. Barry, *Laser Cooling and Slowing of a Diatomic Molecule*, Ph.D. Thesis, Yale University (2013.